



Published in final edited form as:

Endocrine. 2020 January ; 67(1): 95–108. doi:10.1007/s12020-019-02124-3.

Liver derived FGF21 is essential for full adaptation to ketogenic diet but does not regulate glucose homeostasis

Mikiko Watanabe^{1,5,*}, Garima Singhal^{1,*}, ffolliott M Fisher¹, Thomas C Beck², Donald A Morgan³, Fabio Socciarelli⁴, Marie L Mather¹, Renata Risi⁵, Jared Bourke¹, Kamal Rahmouni³, Owen P. McGuinness², Jeffrey S Flier^{1,6}, Eleftheria Maratos-Flier^{1,†}

¹Department of Medicine, Beth Israel Deaconess Medical Center, Harvard Medical School, Boston, MA 02215, USA

²Department of Molecular Physiology and Biophysics, Vanderbilt University School of Medicine Nashville, TN 37232, USA

³Department of Pharmacology, University of Iowa Carver College of Medicine, Iowa City, IA, 52242, USA

⁴Department of Oncology-Pathology, Karolinska Institutet, 171 76 Stockholm, Sweden

⁵Department of Experimental Medicine, Section of Medical Pathophysiology, Food Science and Endocrinology, Sapienza University of Rome, 00161 Rome, Italy

⁶Department of Neurobiology, Harvard Medical School, Boston MA 02215, U.S.A

Abstract

Background: Fibroblast Growth Factor 21 (FGF21) is expressed in several metabolically active tissues, including liver, fat and acinar pancreas, and has pleiotropic effects on metabolic homeostasis. The dominant source of FGF21 in the circulation is the liver.

Objective and Methods: To analyze the physiological functions of hepatic FGF21, we generated a hepatocyte specific knockout model (LKO) by mating albumin-Cre mice with FGF21 flox/flox (fl/fl) mice and challenged it with different nutritional models.

Results: Mice fed a ketogenic diet typically show increased energy expenditure; this effect was attenuated in LKO mice. LKO on KD also developed hepatic pathology and altered hepatic lipid

Terms of use and reuse: academic research for non-commercial purposes, see here for full terms.

[†]Corresponding Author: Eleftheria Maratos-Flier, M.D., Division of Endocrinology, Beth Israel Deaconess Medical Center, Boston, MA 02215 USA, emaratos@bidmc.harvard.edu Tel: 617-735-3289.

^{*}These authors contributed equally

Authors Contributions

MW, GS, FMF, TCB, OPM, JSF and EMF conceived and designed the experiments. MW, GS, JB, MM, TCB, DAM and RR and Vanderbilt MMPC performed the experiments. MW, GS, FMF, TCB, FS, OPM analyzed the data. EMF, JSF, FMF, KR and OPM contributed with reagents/materials/analysis tools/critical revisions. MW, GS and EMF drafted the manuscript.

Conflicts of Interest

The authors have nothing to disclose.

Publisher's Disclaimer: This Author Accepted Manuscript is a PDF file of an unedited peer-reviewed manuscript that has been accepted for publication but has not been copyedited or corrected. The official version of record that is published in the journal is kept up to date and so may therefore differ from this version.

homeostasis. When evaluated using hyperinsulinemic euglycemic clamps, glucose infusion rates, hepatic glucose production and glucose uptake were similar between fl/fl and LKO DIO mice.

Conclusions: We conclude that liver derived FGF21 is important for complete adaptation to ketosis but has a more limited role in the regulation of glycemic homeostasis.

Keywords

Fibroblast Growth Factor 21; Ketogenic Diet; Non-alcoholic Fatty Liver Disease; Cholesterol; Energy Metabolism; Adipose Tissue

1. Introduction

Fibroblast Growth Factor 21 (FGF21) is a relatively new addition to the endocrine FGF subfamily that also includes FGF19, a regulator of bile acid synthesis and secretion[1], and FGF23, a regulator of phosphate metabolism [2, 3]. FGF21 was originally described as a factor that increased glucose uptake in cultured adipocytes in an insulin independent manner via Glut1 [4]. Subsequently, exogenous FGF21 was shown to limit obesity and diabetes by inducing weight loss and reducing plasma glucose and triglycerides systemically in rodents and primates [5–8]. Early studies indicated that FGF21 is induced by both fasting and consumption of a ketogenic diet where it plays a role in the oxidation of fatty acids[9, 10]. However, the biology of FGF21 has proven to be quite complex as it is expressed in multiple organs including liver, fat, and pancreas and has downstream actions on multiple tissues, including the brain. In the brain, FGF21 acts on the paraventricular nucleus of the hypothalamus to regulate sympathetic outflow contributing to activation of brown adipose tissue and browning of white adipose tissue, and thus playing a role in thermogenesis in rodents[11].

In addition to its metabolic functions, FGF21 has anti-fibrotic and anti-inflammatory actions which have been best described in the liver, where it regulates carbohydrate and lipid metabolism as well as fatty acid oxidation under various conditions [9, 12, 13]. Animals consuming diets low in methionine and choline develop a marked induction of FGF21 and lipotoxic changes in the liver, and mice lacking FGF21 show exaggerated inflammation and fibrosis. Similar effects are seen in mice consuming high fructose diets. FGF21 also plays a protective role when liver homeostasis is challenged with other noxious stimuli such as alcohol, acetaminophen, carbon tetrachloride and diethylnitrosamine [12, 14–20].

FGF21 levels in the circulation correlate with levels of its synthesis in the liver and in rodents the liver has been shown as the predominant contributor to circulating FGF21. To better understand the hepatic contribution to systemic FGF21 biology, we generated mice lacking FGF21 expression in hepatocytes (LKO) by mating Alb-Cre mice to FGF21 fl/fl mice. As mice lacking FGF21 have atypical responses to both ketogenic and high fat/high sucrose diets we used these diets as a challenge to LKO to assess the relative contribution of liver derived FGF21 to the systemic response [17, 18, 21].

KD consumption in mice induces a dramatic rise in hepatic FGF21 expression accompanied by increases in circulating FGF21 levels which mediate many of the physiologic adaptations

to the diet including increased energy expenditure and activation of BAT[9, 17, 22–24]. No increase in circulating FGF21 was noted in LKO consuming KD confirming the liver as the source of circulating FGF21. Furthermore, the expected increase in activation of BAT and browning of iWAT was attenuated in LKO mice compared to fl/fl mice. While consumption of KD is not associated with excess morbidity or mortality or liver pathology in normal mice, LKO mice developed steatohepatitis [23], consistent with impaired lipid metabolism in mice lacking liver derived FGF21[17].]

Potent glucose lowering effects of FGF21 administration mediated by improved hepatic and peripheral insulin sensitivity in both lean and obese mice have been reported in acute and chronic studies [25, 26]. Mice lacking FGF21 globally showed worsened glucose tolerance than wild-type animals as assessed by a glucose tolerance test. However, when mice became obese eating a high fat high sucrose diet no difference was seen between WT and global FGF21-KO animals. [21, 27]. A recent report using clamps studies showed that the reduced systemic insulin sensitivity in lean FGF21KO mice can be restored after FGF21 administration [28].

Surprisingly, we found that hepatic FGF21 appears not to be essential for the maintenance of glycemia in lean or obese LKO mice, as they have similar ITT and GTT compared to fl/fl mice. Further, hyperinsulinemic euglycemic clamps performed on obese LKO mice and controls showed similar glucose homeostasis, glucose infusion rates and total glucose flux rates in the two groups.

Taken together, our data suggest that liver derived FGF21 is required for full adaptation to ketosis but is not necessary for the maintenance of normal glucose metabolism.

2. Materials and Methods

2.1 Generation of Liver specific FGF21 KO mice

To generate liver specific FGF21 KO mice C57/Bl6 embryonic stem cell lines containing a construct with the third exon of FGF21 flanked by LoxP sites ($Fgf21^{tm1a(EUCOMM)Hmgu}$) were acquired from “The European Conditional Mouse Mutagenesis Program” [29] and injected into blastocysts of C57/Bl6 female mice by the Beth Israel Deaconess Medical Center Transgenic Core. Offspring were selected by chimeric coat color and bred to ensure germ line transmission. These mice were bred to germ line FLP-FRT mice to remove obsolete elements such as PhosphoGlycerate Kinase (PGK) neo cassette. Offspring were tested for the presence of one complete copy of the FGF21 flox allele, bred to homozygosity and subsequently with albumin-CRE transgenic mice (C57Bl/6J background) to generate LKO mice. Tissue specific recombination of exon 3 of the FGF-21 allele was confirmed by determining that offspring mice expressed the albumin-CRE and did not express exon 3 of the FGF-21 allele. DNA from several tissues was separated by gel electrophoresis and loss of exon 3 only occurred in the liver (data not shown). For the purpose of the experiments herein presented fl/fl littermates were used as WT controls.

2.2 Animal experiments

As previous experiments showed that age can affect metabolic adaptations to stimuli, mid adult male mice (age 10–12 weeks) only were utilized in the herein presented experiments. LKO and C57BL/6J fl/fl littermate mice were split into four groups at about 12 weeks of age and thereafter fed standard chow (n = 18) or KD (n = 32) and remained on their respective diets until the end of the study (9 weeks). For metabolic studies of energy balance and for food intake assessment, they were singly housed with cage enrichment under a 12-hour light, 12-hour dark cycle (06:00 h-18:00 h) and an ambient temperature of 22±2°C.

LabDiet 5008 (Pharmaserv, Framingham, MA) consisting of (6.7% fat (cholesterol 223 mg/kg, 0.02%), 23.6% protein and 56% carbohydrate in the form of starch 29.4%, 2.5% sucrose) kcal by weight was used as standard chow. F3666 (Bioserv, Frenchtown, NJ) consisting of 75.1% fat (cholesterol 880 mg/kg, 0.09%), 8.6% protein, and 3.2% carbohydrate (0% sucrose) by weight was used as KD. Mice had *ad libitum* access to food and water or water alone when fasted. All procedures were conducted in accordance with National Institutes of Health Guidelines for the Care and Use of Animals and were approved by the Institutional Animal Care and Use Committee.

For euthanasia, deep anesthesia was reached through intraperitoneal (IP) injection of ketamine/xylazine (ketamine 1 ml/kg, xylazine 100 µl/kg), mice were then euthanized by cardiac puncture exsanguination and cervical dislocation between 09:00 and 11:00 and rapidly dissected, tissues were harvested, flash frozen in liquid nitrogen and kept at –80° C until analyzed or fixed in 10% formalin for 24 hours for histological studies.

For the HFD study, WT and LKO mice (n=18) were put on a high sucrose high fat diet (Bioserv F3282; 59% fat, 14.9% protein, 26% carbohydrate (%Kcal); cholesterol 345 mg/kg, 0.03%) for 9 weeks and evaluated at the Vanderbilt University Mouse Metabolic Phenotyping center.

2.3 Glucose Tolerance Test

On experimental week 5, mice were fasted for 16 hours before an intraperitoneal injection of D-glucose (2 g/kg body wt; Sigma, St. Louis, MO) at 4 hours after light onset. Tail blood glucose concentrations were measured at 0, 10, 20, 30, 60, 90 and 120 minutes using a handheld glucometer (OneTouch Ultra, Lifescan, Milpitas, CA).

2.4 Insulin Tolerance Test

Mice were fasted for 6 hours on experimental week 6 before an intraperitoneal injection of 0.75 IU/Kg regular insulin (Eli Lilly and Co., Indianapolis, IN). Tail blood glucose concentrations were measured at 0, 15, 30, 60 and 75 minutes using a handheld glucometer (OneTouch Ultra, Lifescan, Milpitas, CA).

2.5 Hyperinsulinemic euglycemic clamp

The study was conducted in the Vanderbilt University Mouse Metabolic Phenotyping Center. The surgical procedures utilized to implant chronic catheters have been described previously [30–32]. Briefly, mice were anesthetized with isoflurane. The left common carotid artery

and right jugular vein were catheterized for sampling and infusing, respectively. Animals were individually housed, and all metabolic experiments were performed following a 5-day postoperative recovery period as previously described. Briefly, conscious, unrestrained mice were fasted at 7:00 (t=-300 min). 2 hours prior to initiation of the clamp a 1 μ Ci bolus of [3-³H]-D-glucose was given into the jugular vein (t=-120 min) followed by a constant infusion at a rate at 0.05 μ Ci/min. Two hours later, a baseline arterial blood sample was drawn and blood glucose, [3-³H]-D-glucose, hematocrit and plasma insulin were measured. A 145 min hyperinsulinemic-euglycemic (4 mU/kg/min) clamp was then initiated. [3-³H]-D-glucose was added to the variable glucose infusion that was used to maintain euglycemia and the constant infusion of [3-³H]-D-glucose was discontinued so as to clamp arterial glucose specific activity at a constant level. At t=80, 90, 100 and 120 min, blood samples were taken to determine [3-³H]-D-glucose specific activity. At t=120 min, a 13 μ Ci bolus of 2-deoxy [¹⁴C] glucose ([2-¹⁴C]DG) was administered into the jugular vein catheter. At t=122, 125, 130, 135, and 145 min arterial blood was sampled to determine blood glucose, plasma [3-³H]-D-glucose and [2-¹⁴C]DG. Arterial insulin concentration was measured at 100 and 120 min. At t=145 min mice were then anesthetized. The soleus, gastrocnemius, white superficial vastus lateralis (Quad), liver, heart, EWAT, IWAT, BAT and brain were excised, immediately frozen in liquid nitrogen, and stored at -70 °C until future tissue analysis. Immunoreactive insulin was assayed using a Rat Radioimmunoassay kit cross-reacting with mice insulin (Perkin Elmer). Tissues and plasma samples were deproteinized as described and used to measure [3-³H]-D-glucose, ([2-¹⁴C]DG and [2-¹⁴C]DG -phosphate ([2-¹⁴C]DGP). Glucose flux rates were assessed using non-steady state equations assuming a volume of distribution (130 ml/kg). Tissue-specific clearance (K_g) of [2-¹⁴C]DG and an index of glucose uptake (R_g) were calculated as previously described [33]: $K_g = [2-^{14}C]DGP_{tissue} / AUC [2-^{14}C]DG_{plasma}$, $R_g = K_g \times [glucose]_{plasma}$, where [2-¹⁴C]DGP_{tissue} is the [2-¹⁴C]DGP radioactivity (dpm/g) in the tissue, AUC [2-¹⁴C]DG_{plasma} is the area under the plasma [2-¹⁴C]DG disappearance curve (dpm/mL/min), and [glucose]_{plasma} is the average blood glucose (μ g/ μ l) during the experimental period (t=102–125 min). Data are presented as mean \pm standard error of the mean (SEM).

2.6 Indirect calorimetry

Mice were maintained on a 12-hour light, 12-hour dark cycle and metabolic rate was measured on experimental week 6 by indirect calorimetry using a Comprehensive Lab Animal Monitoring System (CLAMS, Columbus Instruments) as previously described [34]. Ambulatory activity, O₂ consumption, and CO₂ production were simultaneously determined. Food and water were available *ad libitum*. All mice were acclimatized to monitoring cages for 48 h prior to the beginning of an additional 72 h of hourly automated recordings of physiological parameters, which were averaged and binned to create day and night depictions of metabolic rate.

2.7 Body composition analysis

Body composition was assessed using an EchoMRI 3-in-1 quantitative Nuclear Magnetic Resonance (qNMR) system (Echo Medical Systems, Houston, TX) on experimental week 7. Lean and fat mass were measured in live conscious mice that had *ad libitum* access to food and water.

2.8 Feeding and weight collection

Food intake was measured over a 7-day period towards the end of the study in individually housed mice with cage enrichment and is reported as a daily mean. Body weights were determined weekly using a tabletop scale between 09:00 and 11:00 in ad libitum fed group housed mice.

2.9 Serum Analysis

Blood was collected by cardiac puncture into centrifuge tubes before centrifugation at 10,000 rpm for 15 min. Serum was separated and stored at -80°C . Serum FGF21 and insulin concentrations were measured according to the manufacturer's instructions using quantitative ELISAs specific for mouse FGF21 and insulin (R&D Systems and Crystal Chem, respectively). ALT and AST (Pointe Scientific, Canton, MI), triglycerides, β -hydroxybutyrate, total cholesterol, glucose (StanBio, Boerne, TX) were measured in duplicate using enzyme colorimetric assays.

2.10 Histologic Analysis

Paraffin embedding and sectioning was performed by the HDDC histology core B at BIDMC. Sections ($5\ \mu\text{m}$) were stained with Hematoxylin/Eosin (H&E) or PicroSirius Red (SR). Slides were analyzed in a blinded fashion by an experienced pathologist (F.S.). Each slide was graded based on the Non Alcoholic Fatty Liver Disease (NAFLD) Activity Score [35] that looks at steatosis, inflammation, and ballooning, as well as the Metavir score [36] that assesses the degree of fibrosis.

2.11 Hepatic Lipid Content Analysis

Hepatic lipids were extracted using a modified Folch method [37]. Briefly, approximately 150 mg of liver were homogenized in chloroform:methanol (2:1) and incubated overnight at room temperature. Saline (0.9%) was then added, and each sample was centrifuged for 10 minutes at 2000 g. The upper organic phase was removed, and the lower phase was dehydrated overnight using a vacuum pump. Lipids were then resuspended, and triglycerides and total cholesterol content were determined using colorimetric assays (StanBio, Boerne, TX) and normalized to gram of liver wet weight.

2.12 RNA extraction and quantitative Real Time PCR

RNA was isolated from flash-frozen tissue using a Direct-zol™ RNA MiniPrep (Zymo Research) according to manufacturer's instructions. A deoxyribonuclease (QIAGEN) step to digest the genomic DNA was included. cDNA was made from 500 ng isolated RNA using oligo(dt) and random hexamer primers and reverse transcriptase (QuantiTech RT kit; QIAGEN). Quantitative PCR was performed using the 7900HT (Applied Biosystems) thermal cycler and SYBR Green PCR master mix (Applied Bio-systems). Relative expression of mRNAs was calculated and normalized to levels of 36B4 for all tissues using the 2^{-C_t} method. Primer sequences are available upon request.

2.13 Immunoblot

Brown adipose tissue (BAT) was homogenized in lysis buffer in the presence of protease inhibitors. Protein concentration of the extracts was determined with the Pierce BCA protein assay kit (Thermo Fisher, Waltham, MA). 1 µg of total protein was used for western blots (4–15% Criterion gel, Biorad Laboratories; nitrocellulose, Protran; Schleicher and Schuell, Keene, NH). For Uncoupling Protein 1 (UCP1) immunoblots, membranes were blocked in 5% BSA/0.1% Tween in TBS overnight, and then incubated for 2 hours at room temperature with an anti UCP1 monoclonal antibody (Abcam, Cambridge, UK) diluted 1:10000 in 5% BSA/0.1% Tween in TBS. Histone H3 was used as loading control. The blots were developed using Super Signal West Pico chemiluminescent reagent (Pierce, Rockford, IL). Band intensity was quantified using ImageJ software (U. S. National Institutes of Health, Bethesda, Maryland, USA).

2.14 Sympathetic nerve activity measurements

Measurement of sympathetic nerve activity (SNA) to BAT was performed under anesthesia [induced with Ketamine (91 mg/kg body weight) and Xylazine (9.1 mg/kg body weight) and maintained with α -chloralose (initial dose: 12 mg/kg, then sustaining dose of 6 mg/kg/hr)] with body temperature maintained at 37.5 °C using a heat lamp as previously described on a separate cohort of WT and LKO mice (n=24) [38–40]. SNA was recorded in mice consuming KD for 24 hours or >10 weeks to observe and differentiate an acute and a chronic response to the diet.

2.15 Statistical analysis

All data are given as mean \pm SEM. Statistical analysis was performed using GraphPad Prism 5 software (La Jolla, CA). Significance was determined using either an unpaired two tailed student t-test, two-way ANOVA with repeated measures or two-way ANOVA followed by Bonferroni's post-hoc test where appropriate. Statistical analysis for indirect calorimetry data was performed by analysis of covariance using web-based analysis tool CalR[41] taking into account body mass as covariate. Differences were considered significant at a level of $p < 0.05$. Significance is designated by asterisks with * $P < 0.05$, ** $P < 0.01$, *** $P < 0.001$, **** $P < 0.0001$.

3. Results

3.1 LKO mice demonstrate partial induction of FGF21 in adipose tissue

We first investigated the contribution of liver derived FGF21 to circulating levels upon KD challenge in fl/fl (control) and LKO mice with *ad libitum* access to food and water. Fl/fl mice responded as expected to KD diet with approximately a 75-fold increase in FGF21 serum levels (fl/fl chow 210.5 ± 71.15 pg/ml; vs KD: 15677 ± 3192 pg/ml; $p = 0.0006$). LKO mice showed detectable, although extremely low FGF21 levels at baseline which increased by 4-fold with KD consumption (LKO chow: 40.20 ± 4.35 pg/ml; LKO KD: 161.1 ± 18.55 pg/ml; $p < 0.0001$ Fig 1A). Maximal levels in LKO were lower than baseline levels of fl/fl mice.

Increased serum FGF21 levels in fl/fl mice in response to KD were accompanied by an 88-fold increase in hepatic gene expression. Hepatic mRNA expression of FGF21 in LKO mice remains undetectable under either dietary condition (Fig 1B). This led us to consider that the small upregulation in LKO mice might derive from a possible compensatory contribution to circulating FGF21 from fat or muscle.

We therefore assessed FGF21 gene expression in brown adipose tissue (BAT), epididymal white adipose tissue (EWAT), inguinal white adipose tissue (IWAT) and muscle (Fig 1C). FGF21 expression in BAT is comparable between the genotypes and KD consumption leads to a small increase in expression. Similarly, EWAT and IWAT have comparable FGF21 expression in both groups under chow fed conditions. In EWAT of LKO mice consuming KD, FGF21 expression increased about four-fold but this increase was only 3% of that seen in liver of fl/fl mice. Again, both the groups on KD expressed similar levels of FGF21 in IWAT. FGF21 mRNA expression levels in muscle were unchanged by diet or genotype (Fig 1C). Thus, expression of FGF21 in adipose tissue may contribute to low but detectable serum FGF21 levels in LKO mice.

Expression of mRNA encoding the obligate co-receptor of FGF21 β Klotho (KLB) was assessed in FGF21 target tissues and was found to be significantly decreased in the liver of both KD fed groups as well as brown adipose tissue (Suppl. Fig. 1).

3.2 LKO mice on KD fail to increase energy expenditure resulting in attenuated weight loss.

Next, we assessed the role of liver derived FGF21 in the rise of energy expenditure seen upon KD consumption. When eating chow, fl/fl and KO mice had similar body weights (fl/fl 26.3 ± 2.1 ; LKO 28.5 ± 1.9 ; n.s.) and had similar profiles with regard to energy expenditure, ambulation substrate oxidation preference (supplementary fig 2 B–D). Upon feeding of KD, both KD and fl/fl and LKO mice initially showed a similar degree of weight loss. After two weeks, fl/fl mice continued to lose weight while LKO mice began to gain weight and were significantly heavier from week 8 on (Fig. 2 A). Body composition analysis at week 7 showed that LKO mice accumulated more fat (Fig. 2 B), and lean mass (Suppl. Fig. 1 B) compared to KD fed fl/fl mice despite similar caloric intake in all groups (Suppl. Fig. 1 C).

Energy expenditure was measured after 6 weeks of KD feeding when mice were well adapted to the dietary interventions. Fl/fl mice showed significantly higher energy expenditure as assessed by O₂ consumption (VO₂) in both light and dark cycles, whereas LKO failed to increase VO₂ under the same conditions (Fig. 2 C). Overall ambulatory activity was decreased, to a similar extent, in both fl/fl and LKO mice eating KD compared to the chow diet (Fig. 2 D). We then further investigated the mechanism through which absence of liver derived FGF21 affects energy expenditure. UCP-1 protein levels, an indicator of BAT activation, was attenuated in LKO mice, compared to fl/fl mice fed with KD (Fig. 2 E). Sympathetic nerve activity (SNA) subserving BAT, measured in a separate cohort of mice, was significantly reduced in LKO mice compared to fl/fl littermates consuming KD, measured at two different time points: 24 hours and after 10 weeks (Fig. 2 F, G). This led us to conclude that liver derived FGF21 is important in acting on the brain to

drive the sympathetic outflow that contributes to the activation of brown adipose tissue necessary for thermogenesis.

Both groups of KD fed mice maintained similar ketotic status as assessed by serum β -hydroxybutyrate levels, a well validated index of ketosis (Table 1).

3.3 LKO mice have progressive liver injury and altered lipid metabolism on KD

We then evaluated liver pathology of the experimental animals to ascertain whether liver derived FGF21 is hepatoprotective. Histopathologic analysis of liver Hematoxylin/Eosin and Sirius Red stained specimen from fl/fl mice fed either chow or KD showed normal hepatic histology (Fig. 3 A i–ii, v–vi). However, livers of LKO mice on KD were significantly heavier (Fig. 3 B) and demonstrated increased lobular inflammation and ballooning (Fig 3A vii) with a significantly higher NAFLD score (Fig. 3 C). There was no significant fibrosis in KD fed mice irrespective of the genotype (Fig. 3 B vi, viii; C). Worse liver pathology of KD fed LKO mice was confirmed by elevated Alanine aminotransferase (ALT) serum levels (Table 1). Triglycerides content did not differ between diet matched littermates but was significantly elevated in KD compared to chow fed groups (Fig. 3 D). On the contrary, cholesterol content was increased in KD fed LKO mice compared to fl/fl (Fig. 3 E), suggesting that liver derived FGF21 may be linked to altered cholesterol metabolism.

Hepatic gene expression markers for inflammation, fibrosis and lipid metabolism were also measured (Fig 4 A). TIMP1 and MMP2 were significantly induced in LKO mice on KD compared to diet matched fl/fl littermates, while several other genes were comparable in both the KD fed groups (Fig. 4 A–B).

Hepatic gene expression analysis revealed a significant reduction of lipogenic genes with consumption of KD (Fig. 4 C) irrespective of genotype. However, induction of genes involved in lipid transport and fatty acid oxidation were attenuated in LKO including CD36, LCAD, VLCAD, ACOX1 and CPT1 α (Fig. 4 C). Further, PPAR-coactivators PGC1 α and PGC1 β were also significantly lower in these mice, consistent with data from FGF21KO mice [17] (Fig. 4 D).

Moreover, hypercholesterolemia (Table 1) in KD fed LKO mice was noted. We therefore further investigated the role of hepatic FGF21 in cholesterol metabolism and found that its absence was associated with reduced expression of genes involved in cholesterol excretion into bile such as ABCG5, ABCG8, LXR, Cyp7A1, SHP, suggesting impaired cholesterol clearance in these mice (Fig. 4 E). Endogenous biosynthesis of cholesterol also appeared to be reduced in KD fed LKO as HMGCS1, HMGCR, and SREBP2 gene expression were downregulated. Proprotein convertase subtilisin/kexin type 9 (PCSK9) and LDL Receptor (LDLR) were both found to be profoundly decreased in these mice compared to all other groups (Suppl. Fig. 1 D).

3.4 Glucose metabolism is not impaired in obese LKO mice

Finally, we investigated the role of liver derived FGF21 in glucose metabolism. LKO mice showed no impairment in glucose metabolism on chow as measured by ipGTT and Insulin Tolerance Test (ITT) compared to WT mice (Suppl. Fig 2E–F). When fed HFD for 16 weeks

both fl/fl and LKO gained weight and maintained very similar GTT responses (Suppl. Fig 2 G). Hyperinsulinemic euglycemic clamps were performed on these mice. Glucose levels were clamped at ~120 mg/dl to maintain euglycemia (Fig 5A). No significant difference was seen in the glucose infusion rate (GIR; $\text{mg}\cdot\text{kg}^{-1}\cdot\text{min}^{-1}$) (Fig 5B). Similar plasma insulin and total glucose flux at baseline and during the clamp were also observed (Fig 5 C–D). Endogenous glucose production was very low in both groups indicating suppression of liver glucose production by insulin (Fig 5 E). Insulin-stimulated glucose uptake in multiple tissues did not differ between the fl/fl and LKO groups (Fig 5 F). Altogether, our data suggest that loss of hepatic FGF21 does not affect glucose metabolism on any of the investigated conditions.

4 Discussion

FGF21 regulates energy homeostasis and has beneficial metabolic effects including weight loss and improved glycemia in humans and mice [5, 6]. However, the physiology of FGF21 is very complex as it derives from multiple tissues and exerts metabolic functions via three modes of action: autocrine, paracrine, and endocrine [42, 43]. Hepatic FGF21 is the major source of circulating FGF21 which is responsible for endocrine actions. To better differentiate the relative endocrine aspects of FGF21 action compared to autocrine/paracrine actions we generated a hepatocyte specific FGF21 deficient mouse model, designated as LKO mice. Deletion of hepatic FGF21 resulted in an 80% reduction in serum FGF21 levels at baseline; levels did not increase with fasting, a perturbation that reliably lead to a significant rise in FGF21 (Suppl Fig 2A). Ketogenic diet serve as nutritional challenge, and in mice induce a massive increase in hepatic FGF21 expression and increased circulatory levels with substantial physiologic changes including increased energy expenditure and sympathetic outflow [23, 24] [44, 45]. In LKO consuming KD, the hepatic induction of FGF21 is absent and there is marked attenuation of SNS outflow, demonstrated by direct measurement of sympathetic nerve activity.

We previously reported that mice with systemic FGF21 deletion failed to demonstrate any weight loss response to KD and indeed gained weight rather than the attenuated weight loss we observed in LKO mice. Given the report of Stemmer and the difference in our own results, we re-examined the effect of KD consumption in global FGF21 KO under the same conditions described here used in LKO mice. In particular, our original study was performed in older mice housed in a non-barrier facility [17]. Although weight loss was observed in our repeat study it was no longer as dramatic as we previously reported (Suppl. Fig. 3 A). However, in this repeat study with global FGF21 KO mice, the pattern of energy expenditure pattern was as described in the previous study (Suppl. Fig 3 B–C). This reinforces the key role of FGF21 in KD induced energy expenditure. However, weight loss may be variable depending on other factors such as age, duration of the studies and housing details.

LKO mice have higher cholesterol levels in both serum and liver. It is to be noted that the cholesterol content of KD is 3 times higher than chow diet (KD 62.5 mg/kg vs chow 21 mg/Kg). In the presence of FGF21 the increased dietary cholesterol leads to upregulation of cholesterol clearance as indicated by increased expression of clearance markers; these markers are not induced in LKO mice. However, cholesterol biosynthesis and uptake are also

reduced, effects that may reflect a physiological feedback response to both the high dietary cholesterol and the impaired clearance [46–48]. FGF21 is also viewed as a negative regulator of bile acid synthesis in a Cyp7a1 dependent pathway [49, 50]. Reduced activity of this pathway leads to increased cholesterol in the gut. LKO show reduced gene expression of markers of bile acid synthesis, consistent with the suggested link between FGF21 and bile acids metabolism, possibly in a Cyp7a1 independent manner as the latter remains unchanged.

We have previously reported that WT mice fed a KD develop mild liver inflammation and fibrosis, although this does not decrease their lifespan [23]. We have also reported that FGF21KO mice consuming an MCD diet show more severe liver steatosis, inflammation and fibrosis compared to WT mice [12]. Our findings here in LKO mice consuming KD are consistent with a protective effect of hepatic-derived FGF21 on the liver as fl/fl mice consuming KD had no histopathologic changes in contrast to LKO mice. Liver injury, reflected in increased ballooning and inflammation, may not only be consequent to fat (triglycerides) deposition, but also to a direct cytotoxic effect of cholesterol through modifications of signaling pathways and disruption of intracellular structures and membrane fluidity [51]. Whether this may lead to liver failure, hepatocellular carcinoma or decreased life expectancy needs to be further explored with more long-term studies.

Exogenous FGF21 suppresses hepatic glucose production and stimulates peripheral glucose uptake in obese mice [5, 8, 25, 26]. In the obese state, FGF21 is increased. However, FGF21 does not play an essential role in obesity-induced changes in GTT or ITT as we show that these are the same in both obese WT mice and mice with global FGF21 deletion [21, 27]. Moreover, we found that BAT glucose uptake was unaffected during the clamp. Similarly, we found that deletion of hepatic FGF21 had no effect on glycemia irrespective of the dietary conditions, including chow, HFD and KD. This suggests that FGF21 is dispensable with regard to glucose homeostasis under these conditions. This is in contrast to some previously published reports. Markan et al. have shown that liver derived FGF21 is responsible for glucose disposal into BAT and improving insulin sensitivity in mice [52]. Another report suggests that hepatic FGF21 deficiency promotes metabolic syndrome as in that report HFD-fed LKO mice were significantly more glucose intolerant, more insulin resistant, and more pyruvate intolerant than HFD-fed control mice [53]. We did not observe any difference in the phenotype of glucose at baseline and have no specific explanation for this discrepancy. However, it is difficult to cross compare dietary studies among various facilities in mouse models conducted by different investigators [54]. Differences may reflect diet formulation, duration of the studies and details of housing conditions [55]. However, the differences observed among studies suggest that the effect of hepatic derived FGF21 deficiency on glucose metabolism is not straight forward.

Collectively, our data demonstrate that liver derived FGF21, despite being the largest source of endocrine FGF21 is not necessary for normal glucose metabolism but is required as an endocrine factor mediating the full adaptation to ketosis. The effect of liver-derived FGF21 is hepatoprotective, as seen with progressive liver injury upon KD consumption. The lipid lowering effect of FGF21 may be due in part to its permissive role in cholesterol excretion

that our findings suggest for the first time, but further studies are warranted to confirm this observation.

Supplementary Material

Refer to Web version on PubMed Central for supplementary material.

Acknowledgments

We thank Dr Pavlos Pissios for scientific discussions and Dr Thomas Webb for technical assistance.

Financial support

This work was supported by NIH Grant DK028082 (to E.M.F. and J.S.F.). M.W. was supported by funds from The Rotary Club of Rome. We are grateful for the help from the HDDC Core supported by NIH Grant NIDDK P30 DK034854. Generation of genetically altered floxed mice was made under the auspices of BADERC 5P30DK057521 and the BNORC 5P30DK046200. K.R was supported by funds from the NIH (HL084207), the American Heart Association (14EIA18860041) and the University of Iowa Fraternal Order of Eagles Diabetes Research Center. O.P.M. was supported by funds from the NIH (DK059637). The Vanderbilt Mouse Metabolic Phenotyping Center (DK059637) and the Hormone Assay and Analytical Services Core (DK059637 and DK020593) provided surgical and analytical support for clamp studies.

Abbreviations

FGF21

Fibroblast Growth Factor 21

f1/f1

FGF21 Flox/flox

LKO

Lver specific Knockout

KD

Ketogenic Diet

HFD

High Fat Diet

PPAR α

Peroxisome Proliferator-Activated Receptor α

FGF21KO

Fibroblast Growth Factor 21 Knockout

WT

Wild Type

IP

Intra Peritoneal

([2-¹⁴C]D-G) [2-¹⁴C]D

Glucose

RG

Glucose metabolic Index

SEM

Standard Error of the Mean

CLAMS

Comprehensive Lab Animal Monitoring System Oxymax

qNMR

Quantitative Nuclear Magnetic Resonance

ALT

Alanine aminotransferase

PGK

PhosphoGlycerate Kinase

NAFLD

Non-Alcoholic Fatty Liver Disease

BAT

Brown adipose tissue

UCP1

Uncoupling Protein 1

SNA

Sympathetic Nerve Activity

ANOVA

Analysis Of Variance

KLB

β -Klotho

EWAT

Epididymal White Adipose Tissue

IWAT

Inguinal White Adipose Tissue

ipGTT

Intraperitoneal Glucose Tolerance Test

ITT

Insulin Tolerance Test

RER

Respiratory Exchange Ratio

MCD

Methionine Choline Deficient

SNS

Sympathetic Nervous System

DIO

Diet Induced Obesity

FAS

Fatty Acids Synthase

SCD-1

Stearoyl-CoA desaturase

CD36

Cluster of Differentiation 36

LCAD

Long Chain Acyl-CoA dehydrogenase

VLCAD

Very Long Chain Acyl-CoA dehydrogenase

ACOX1

Peroxisomal acyl-coenzyme A oxidase 1

CPT1 α Carnitine palmitoyltransferase I α **PPAR**Peroxisome proliferator-activated receptor γ Coactivator 1 α PGC1 α **PGC1 β** Peroxisome proliferator-activated receptor (PPAR) γ Coactivator 1 β **ABCG5**

ATP-Binding Cassette subfamily G member 5

ABCG8

ATP-Binding Cassette sub-family G member 8

LXR

Liver X Receptor

Cyp7A1

Cytochrome P450 7A1

SHP

Small Heterodimer Partner

HMGCS1

3-Hydroxy-3-MethylGlutaryl-CoA Synthase

HMGCR

3-Hydroxy-3-MethylGlutaryl-CoA Reductase

SREBP2

Sterol Regulatory Element-Binding Protein 2

FCSK9

Proprotein Convertase Subtilisin/Kex in type 9

LDLR

LDL Receptor

TGF1 β Transforming growth factor 1 β **MCP1**

Monocyte chemoattractant protein-1

MMP2

Matrix MetalloProteinase-2

SMA

Smooth Muscle Actin

IL1 β Interleukin 1 β **TIMP**

metallopeptidase inhibitor 1.

References

- [1]. Inagaki T, Choi M, Moschetta A, Peng L, Cummins CL, McDonald JG, et al., 2005. Fibroblast growth factor 15 functions as an enterohepatic signal to regulate bile acid homeostasis. *Cell Metab* 2, 217–225. [PubMed: 16213224]
- [2]. Shimada T, Mizutani S, Muto T, Yoneya T, Hino R, Takeda S, et al., 2001. Cloning and characterization of FGF23 as a causative factor of tumor-induced osteomalacia. *Proc Natl Acad Sci U S A* 98, 6500–6505. [PubMed: 11344269]
- [3]. Shimada T, Yamazaki Y, Takahashi M, Hasegawa H, Urakawa I, Oshima T, et al., 2005. Vitamin D receptor-independent FGF23 actions in regulating phosphate and vitamin D metabolism. *Am J Physiol Renal Physiol* 289, F1088–1095. [PubMed: 15998839]
- [4]. Kharitonov A, Shiyanova TL, Koester A, Ford AM, Micanovic R, Galbreath EJ, et al., 2005. FGF-21 as a novel metabolic regulator. *The Journal of clinical investigation* 115, 1627–1635. [PubMed: 15902306]

- [5]. Coskun T, Bina HA, Schneider MA, Dunbar JD, Hu CC, Chen Y, et al., 2008. Fibroblast growth factor 21 corrects obesity in mice. *Endocrinology* 149, 6018–6027. [PubMed: 18687777]
- [6]. Gaich G, Chien JY, Fu H, Glass LC, Deeg MA, Holland WL, et al., 2013. The effects of LY2405319, an FGF21 analog, in obese human subjects with type 2 diabetes. *Cell metabolism* 18, 333–340. [PubMed: 24011069]
- [7]. Talukdar S, Zhou Y, Li D, Rossulek M, Dong J, Somayaji V, et al., 2016. A Long-Acting FGF21 Molecule, PF-05231023, Decreases Body Weight and Improves Lipid Profile in Non-human Primates and Type 2 Diabetic Subjects. *Cell Metab* 23, 427–440. [PubMed: 26959184]
- [8]. Xu J, Stanislaus S, Chinookoswong N, Lau YY, Hager T, Patel J, et al., 2009. Acute glucose-lowering and insulin-sensitizing action of FGF21 in insulin-resistant mouse models--association with liver and adipose tissue effects. *American journal of physiology. Endocrinology and metabolism* 297, E1105–1114. [PubMed: 19706786]
- [9]. Badman MK, Pissios P, Kennedy AR, Koukos G, Flier JS, and Maratos-Flier E, 2007. Hepatic fibroblast growth factor 21 is regulated by PPARalpha and is a key mediator of hepatic lipid metabolism in ketotic states. *Cell Metab* 5, 426–437. [PubMed: 17550778]
- [10]. Inagaki T, Dutchak P, Zhao G, Ding X, Gautron L, Parameswara V, et al., 2007. Endocrine regulation of the fasting response by PPARalpha-mediated induction of fibroblast growth factor 21. *Cell Metab* 5, 415–425. [PubMed: 17550777]
- [11]. Schwenger KJP, Fischer SE, Jackson TD, Okrainec A, and Allard JP, 2018. Non-alcoholic Fatty Liver Disease in Morbidly Obese Individuals Undergoing Bariatric Surgery Prevalence and Effect of the Pre-Bariatric Very Low Calorie Diet. *Obes Surg* 28, 1109–1116. [PubMed: 29098545]
- [12]. Fisher FM, Chui PC, Nasser IA, Popov Y, Cunniff JC, Lundasen T, et al., 2014. Fibroblast growth factor 21 limits lipotoxicity by promoting hepatic fatty acid activation in mice on methionine and choline-deficient diets. *Gastroenterology* 147, 1073–1083 e1076. [PubMed: 25083607]
- [13]. Potthoff MJ, Inagaki T, Satapati S, Ding X, He T, Goetz R, et al., 2009. FGF21 induces PGC-1alpha and regulates carbohydrate and fatty acid metabolism during the adaptive starvation response. *Proc Natl Acad Sci U S A* 106, 10853–10858. [PubMed: 19541642]
- [14]. Desai BN, Singhal G, Watanabe M, Stevanovic D, Lundasen T, Fisher FM, et al., 2017. Fibroblast growth factor 21 (FGF21) is robustly induced by ethanol and has a protective role in ethanol associated liver injury. *Molecular metabolism* 6, 1395–1406. [PubMed: 29107287]
- [15]. Dushay JR, Toschi E, Mitten EK, Fisher FM, Herman MA, and Maratos-Flier E, 2015. Fructose ingestion acutely stimulates circulating FGF21 levels in humans. *Mol Metab* 4, 51–57. [PubMed: 25685689]
- [16]. Fisher FM, Kim M, Doridot L, Cunniff JC, Parker TS, Levine DM, et al., 2017. A critical role for ChREBP-mediated FGF21 secretion in hepatic fructose metabolism. *Molecular metabolism* 6, 14–21. [PubMed: 28123933]
- [17]. Badman MK, Koester A, Flier JS, Kharitonov A, and Maratos-Flier E, 2009. Fibroblast growth factor 21-deficient mice demonstrate impaired adaptation to ketosis. *Endocrinology* 150, 4931–4940. [PubMed: 19819944]
- [18]. Singhal G, Kumar G, Chan S, Fisher FM, Ma Y, Vardeh HG, et al., 2018. Deficiency of fibroblast growth factor 21 (FGF21) promotes hepatocellular carcinoma (HCC) in mice on a long term obesogenic diet. *Mol Metab*.
- [19]. Huang S, He J, Zhang X, Bian Y, Yang L, Xie G, et al., 2006. Activation of the hedgehog pathway in human hepatocellular carcinomas. *Carcinogenesis* 27, 1334–1340. [PubMed: 16501253]
- [20]. Ye D, Wang Y, Li H, Jia W, Man K, Lo CM, et al., 2014. Fibroblast growth factor 21 protects against acetaminophen-induced hepatotoxicity by potentiating peroxisome proliferator-activated receptor coactivator protein-1alpha-mediated antioxidant capacity in mice. *Hepatology* 60, 977–989. [PubMed: 24590984]
- [21]. Singhal G, Fisher FM, Chee MJ, Tan TG, El Ouaamari A, Adams AC, et al., 2016. Fibroblast Growth Factor 21 (FGF21) Protects against High Fat Diet Induced Inflammation and Islet Hyperplasia in Pancreas. *PLoS One* 11, e0148252.

- [22]. Badman MK, Kennedy AR, Adams AC, Pissios P, and Maratos-Flier E, 2009. A very low carbohydrate ketogenic diet improves glucose tolerance in ob/ob mice independently of weight loss. *Am J Physiol Endocrinol Metab* 297, E1197–1204. [PubMed: 19738035]
- [23]. Douris N, Melman T, Pecherer JM, Pissios P, Flier JS, Cantley LC, et al., 2015. Adaptive changes in amino acid metabolism permit normal longevity in mice consuming a low-carbohydrate ketogenic diet. *Biochim Biophys Acta* 1852, 2056–2065. [PubMed: 26170063]
- [24]. Kennedy AR, Pissios P, Otu H, Roberson R, Xue B, Asakura K, et al., 2007. A high-fat, ketogenic diet induces a unique metabolic state in mice. *Am J Physiol Endocrinol Metab* 292, E1724–1739. [PubMed: 17299079]
- [25]. Berglund ED, Li CY, Bina HA, Lynes SE, Michael MD, Shanafelt AB., et al., 2009. Fibroblast growth factor 21 controls glycemia via regulation of hepatic glucose flux and insulin sensitivity. *Endocrinology* 150, 4084–4093. [PubMed: 19470704]
- [26]. Camporez JP, Jornayvaz FR, Petersen MC, Pesta D, Guigni BA, Serr J, et al., 2013. Cellular mechanisms by which FGF21 improves insulin sensitivity in male mice. *Endocrinology* 154, 3099–3109. [PubMed: 23766126]
- [27]. Fisher FM, Chui PC, Antonellis PJ, Bina HA, Kharitonov A, Flier JS, et al., 2010. Obesity is a fibroblast growth factor 21 (FGF21)-resistant state. *Diabetes* 59, 2781–2789. [PubMed: 20682689]
- [28]. Li H, Wu G, Fang Q, Zhang M, Hui X, Sheng B, et al., 2018. Fibroblast growth factor 21 increases insulin sensitivity through specific expansion of subcutaneous fat. *Nat Commun* 9, 272. [PubMed: 29348470]
- [29]. [https://www.mousephenotype.org/data/alleles/MGI:1861377/tm1a\(EUCOMM\)Hmgu](https://www.mousephenotype.org/data/alleles/MGI:1861377/tm1a(EUCOMM)Hmgu). Last access: June 19th 2019
- [30]. Ayala JE, Bracy DP, Malabanan C, James FD, Ansari T, Fueger PT, et al., 2011. Hyperinsulinemic-euglycemic clamps in conscious, unrestrained mice. *J Vis Exp*.
- [31]. Ayala JE, Bracy DP, McGuinness OP, and Wasserman DH, 2006. Considerations in the design of hyperinsulinemic-euglycemic clamps in the conscious mouse. *Diabetes* 55, 390–397. [PubMed: 16443772]
- [32]. Mulligan KX, Morris RT, Otero YF, Wasserman DH, and McGuinness OP, 2012. Disassociation of muscle insulin signaling and insulin-stimulated glucose uptake during endotoxemia. *PLoS One* 7, e30160.
- [33]. Kraegen EW, James DE, Jenkins AB., and Chisholm DJ, 1985. Dose-response curves for in vivo insulin sensitivity in individual tissues in rats. *Am J Physiol* 248, E353–362. [PubMed: 3883806]
- [34]. Singhal G, Douris N, Fish AJ., Zhang X, Adams AC, Flier JS, et al., 2016. Fibroblast growth factor 21 has no direct role in regulating fertility in female mice. *Mol Metab* 5, 690–698. [PubMed: 27656406]
- [35]. Brunt EM, Kleiner DE, Wilson LA, Belt P, Neuschwander-Tetri BA, and Network NCR, 2011. Nonalcoholic fatty liver disease (NAFLD) activity score and the histopathologic diagnosis in NAFLD: distinct clinicopathologic meanings. *Hepatology* 53, 810–820. [PubMed: 21319198]
- [36]. Martinez SM, Crespo G, Navasa M, and Forns X, 2011. Noninvasive assessment of liver fibrosis. *Hepatology* 53, 325–335. [PubMed: 21254180]
- [37]. Folch J, Lees M, and Sloane Stanley GH, 1957. A simple method for the isolation and purification of total lipides from animal tissues. *J Biol Chem* 226, 497–509. [PubMed: 13428781]
- [38]. Seoane-Collazo P, Roa J, Rial-Pensado E, Linares-Pose L, Beiroa D, Ruiz-Pino F, et al., 2018. SF1-Specific AMPK α 1 Deletion Protects Against Diet-Induced Obesity. *Diabetes* 67, 2213–2226. [PubMed: 30104247]
- [39]. Guilherme A, Pedersen DJ, Henriques F, Bedard AH., Henchey E, Kelly M, et al., 2018. Neuronal modulation of brown adipose activity through perturbation of white adipocyte lipogenesis. *Mol Metab* 16, 116–125. [PubMed: 30005879]
- [40]. Shinohara K, Nakagawa P, Gomez J, Morgan DA, Littlejohn NK, Folchert MD, et al., 2017. Selective Deletion of Renin-b in the Brain Alters Drinking and Metabolism. *Hypertension* 70, 990–997. [PubMed: 28874461]

- [41]. Mina AI, LeClair RA, LeClair KB, Cohen DE, Lantier L, and Banks AS., 2018. CalR: A Web-Based Analysis Tool for Indirect Calorimetry Experiments. *Cell Metab* 28, 656–666 e651. [PubMed: 30017358]
- [42]. Fisher FM, and Maratos-Flier E, 2016. Understanding the Physiology of FGF21. *Annu Rev Physiol* 78, 223–241. [PubMed: 26654352]
- [43]. Kharitonov A, and DiMarchi R, 2015. FGF21 Revolutions: Recent Advances Illuminating FGF21 Biology and Medicinal Properties. *Trends Endocrinol Metab* 26, 608–617. [PubMed: 26490383]
- [44]. Douris N, Stevanovic DM, Fisher FM, Cisu TI, Chee MJ, Nguyen NL, et al., 2015. Central Fibroblast Growth Factor 21 Browns White Fat via Sympathetic Action in Male Mice. *Endocrinology* 156, 2470–2481. [PubMed: 25924103]
- [45]. Fisher FM, Kleiner S, Douris N, Fox EC, Mepani RJ, Verdeguer F, et al., 2012. FGF21 regulates PGC-1 α and browning of white adipose tissues in adaptive thermogenesis. *Genes Dev* 26, 271–281. [PubMed: 22302939]
- [46]. Kalaany NY, and Mangelsdorf DJ, 2006. LXRS and FXR: the yin and yang of cholesterol and fat metabolism. *Annu Rev Physiol* 68, 159–191. [PubMed: 16460270]
- [47]. Luu W, Sharpe LJ, Gelissen IC, and Brown AJ., 2013. The role of signalling in cellular cholesterol homeostasis. *IUBMB Life* 65, 675–684. [PubMed: 23847008]
- [48]. Ye J, and DeBose-Boyd RA, 2011. Regulation of cholesterol and fatty acid synthesis. *Cold Spring Harb Perspect Biol* 3.
- [49]. Chen MM, Hale C, Stanislaus S, Xu J, and Veniant MM, 2018. FGF21 acts as a negative regulator of bile acid synthesis. *J Endocrinol* 237, 139–152. [PubMed: 29615519]
- [50]. Zhang J, Gupte J, Gong Y, Weiszmann J, Zhang Y, Lee KJ, et al., 2017. Chronic Over-expression of Fibroblast Growth Factor 21 Increases Bile Acid Biosynthesis by Opposing FGF15/19 Action. *EBioMedicine* 15, 173–183. [PubMed: 28041926]
- [51]. Tabas I, 2002. Consequences of cellular cholesterol accumulation: basic concepts and physiological implications. *J Clin Invest* 110, 905–911. [PubMed: 12370266]
- [52]. Markan KR, Naber MC, Ameka MK, Anderegg MD, Mangelsdorf DJ, Kliewer SA, et al., 2014. Circulating FGF21 is liver derived and enhances glucose uptake during refeeding and overfeeding. *Diabetes* 63, 4057–4063. [PubMed: 25008183]
- [53]. Vernia S, Cavanagh-Kyros J, Barrett T, Tournier C, and Davis RJ, 2016. Fibroblast Growth Factor 21 Mediates Glycemic Regulation by Hepatic JNK. *Cell Rep* 14, 2273–2280. [PubMed: 26947074]
- [54]. Flier JS, 2017. Irreproducibility of published bioscience research: Diagnosis, pathogenesis and therapy. *Mol Metab* 6, 2–9. [PubMed: 28123930]
- [55]. Drucker DJ, 2016. Never Waste a Good Crisis: Confronting Reproducibility in Translational Research. *Cell Metab* 24, 348–360. [PubMed: 27626191]

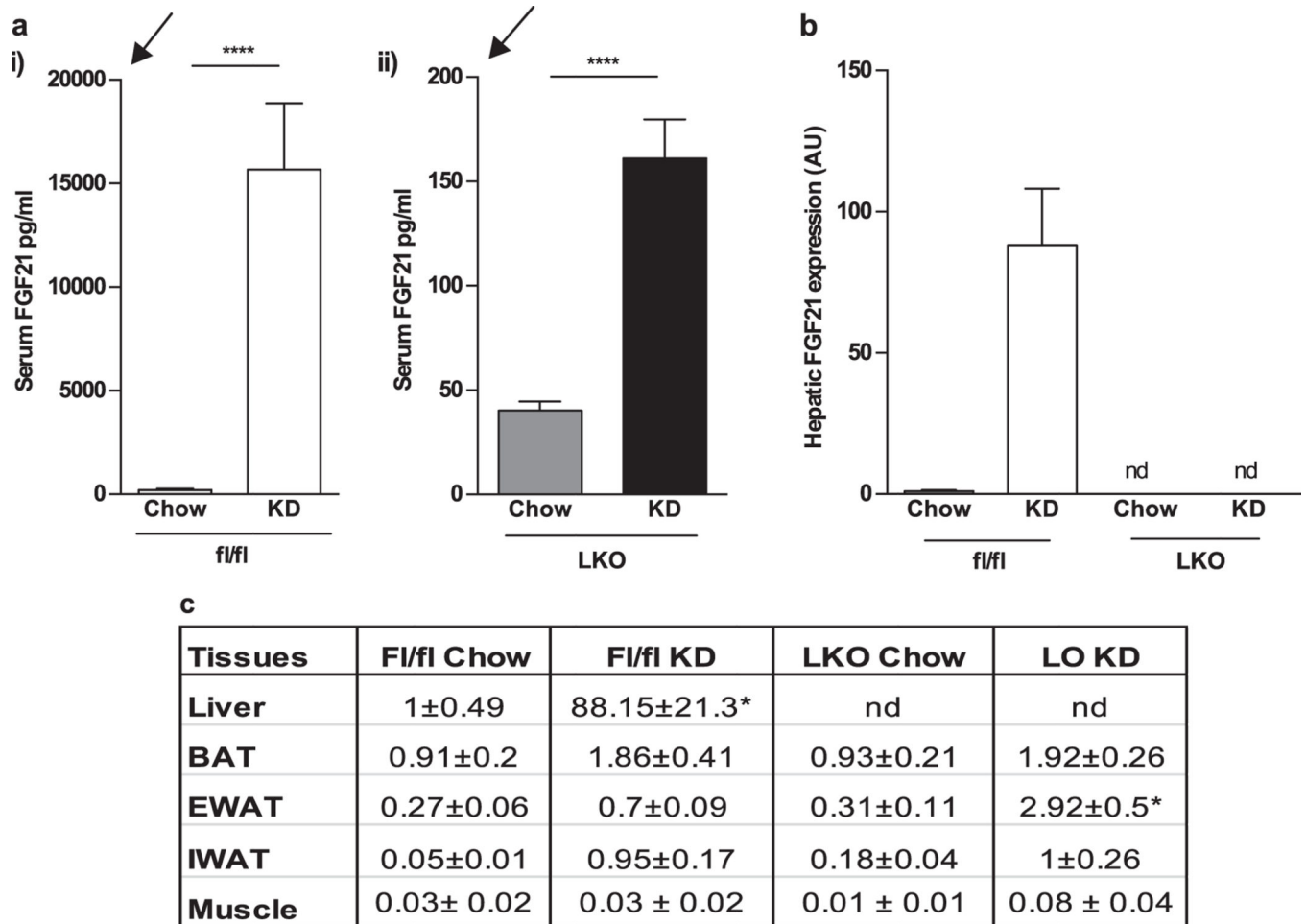


Figure 1.

LKO mice demonstrate partial induction of FGF21 in adipose tissue FGF21 circulating levels and gene expression in fl/fl and LKO mice fed with chow and KD. **a** Circulating FGF21 is significantly induced in fl/fl mice with KD consumption and ad libitum access to food and water. In LKO mice, FGF21 is detectable at low levels at baseline and is induced 4-fold with KD. The arrows highlight the differences in Y axes: LKO KD represents a tiny fraction compared to fl/fl KD. **b** FGF21 gene expression in liver from fl/fl and LKO mice is shown. The FGF21 expression is not detectable in LKO mice. **c** FGF21 expression is detected in adipose depots, including BAT, eWAT and IWAT at baseline, and small inductions are seen with KD. LKO mice show a specific increase in FGF21 in EWAT with KD consumption. FGF21 gene expression in all the tissues is normalized to the hepatic expression of chow-fed fl/fl mice. $N = 7-8$ mice/group. Nd: not detectable. *Significantly different compared to all other groups

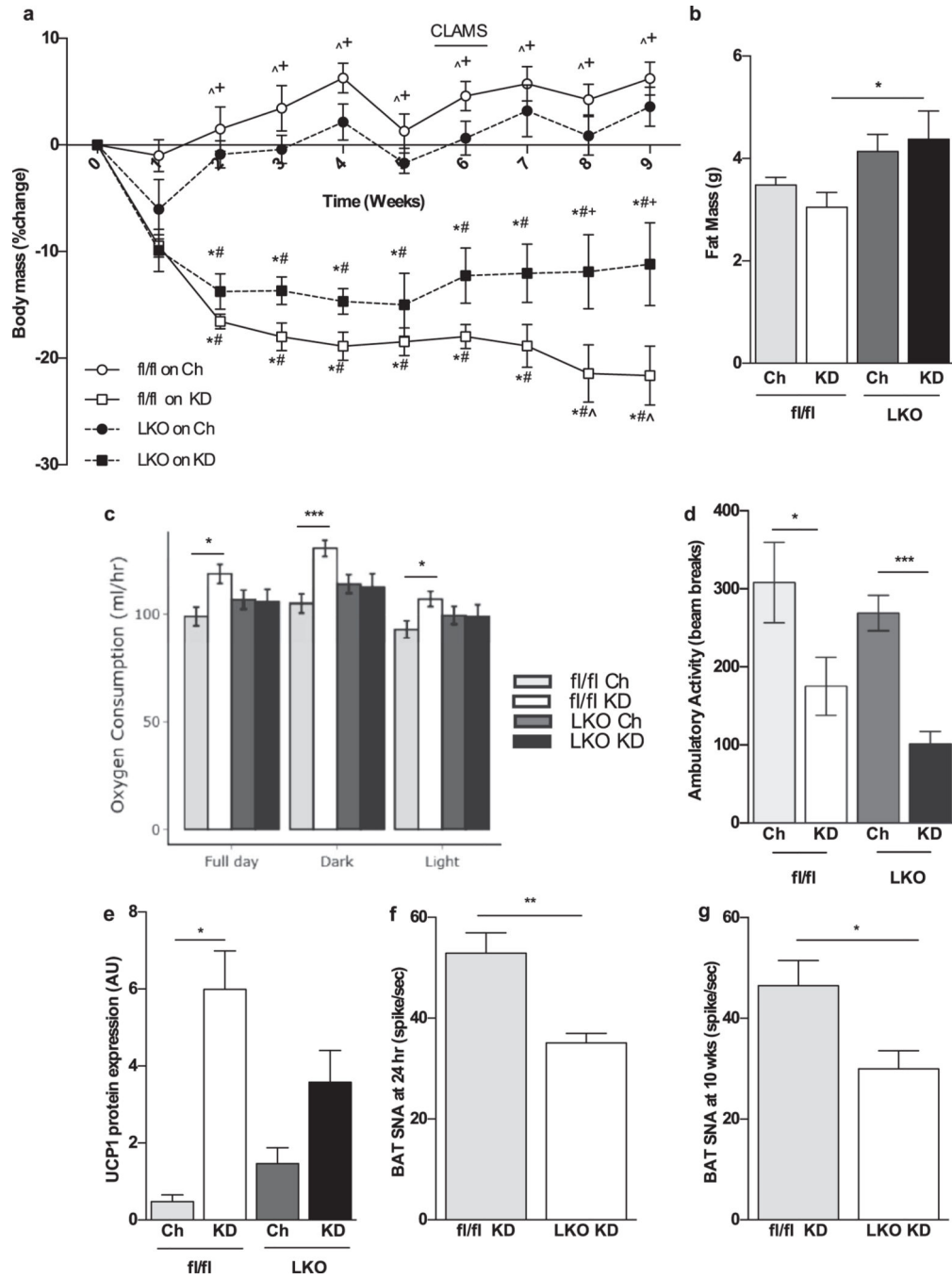


Figure 2. LKO mice show attenuated weight loss on KD relative to chow diet as they fail to increase energy expenditure. **a** A reduction in body weight of KD-fed fl/fl and LKO mice becomes significantly different from week 8 onwards. Absolute baseline body weight was not significantly different among groups (fl/fl Ch 26.3±2.1; fl/fl KD 28.3±1.9; LKO Ch 28.5±1.9; LKO KD 29.5±2.7). **b** KD-fed LKO mice maintain more fat mass. **c** fl/fl mice consuming KD for 6 weeks had significant increase in VO₂ during both dark and light cycle, reflecting a higher energy expenditure that LKO fail to achieve. **d** Ambulatory activity is

reduced with KD consumption in both groups. **e** UCP1 protein is induced in fl/fl mice consuming KD, while this induction is attenuated in LKO mice. **f, g** Sympathetic nerve activity in BAT, both at 24 h and 10 weeks of KD feeding, is reduced in LKO mice compared to fl/fl counterparts. *Significantly different from chow-fed WT; #significantly different from chow-fed LKO; +significantly different from KD-fed WT; ^significantly different from KD-fed LKO. *N* = 6–8 mice/group

Author Manuscript

Author Manuscript

Author Manuscript

Author Manuscript

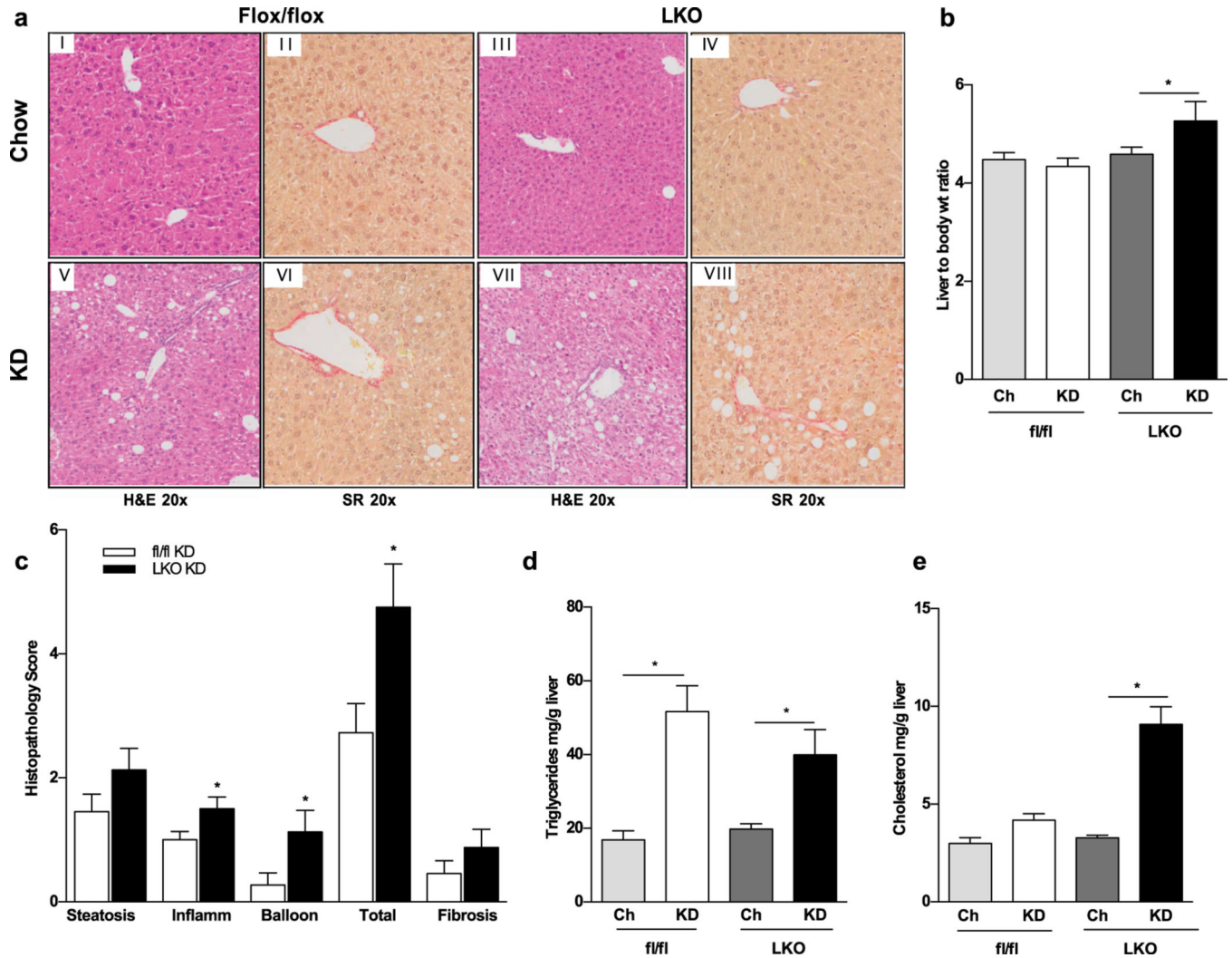
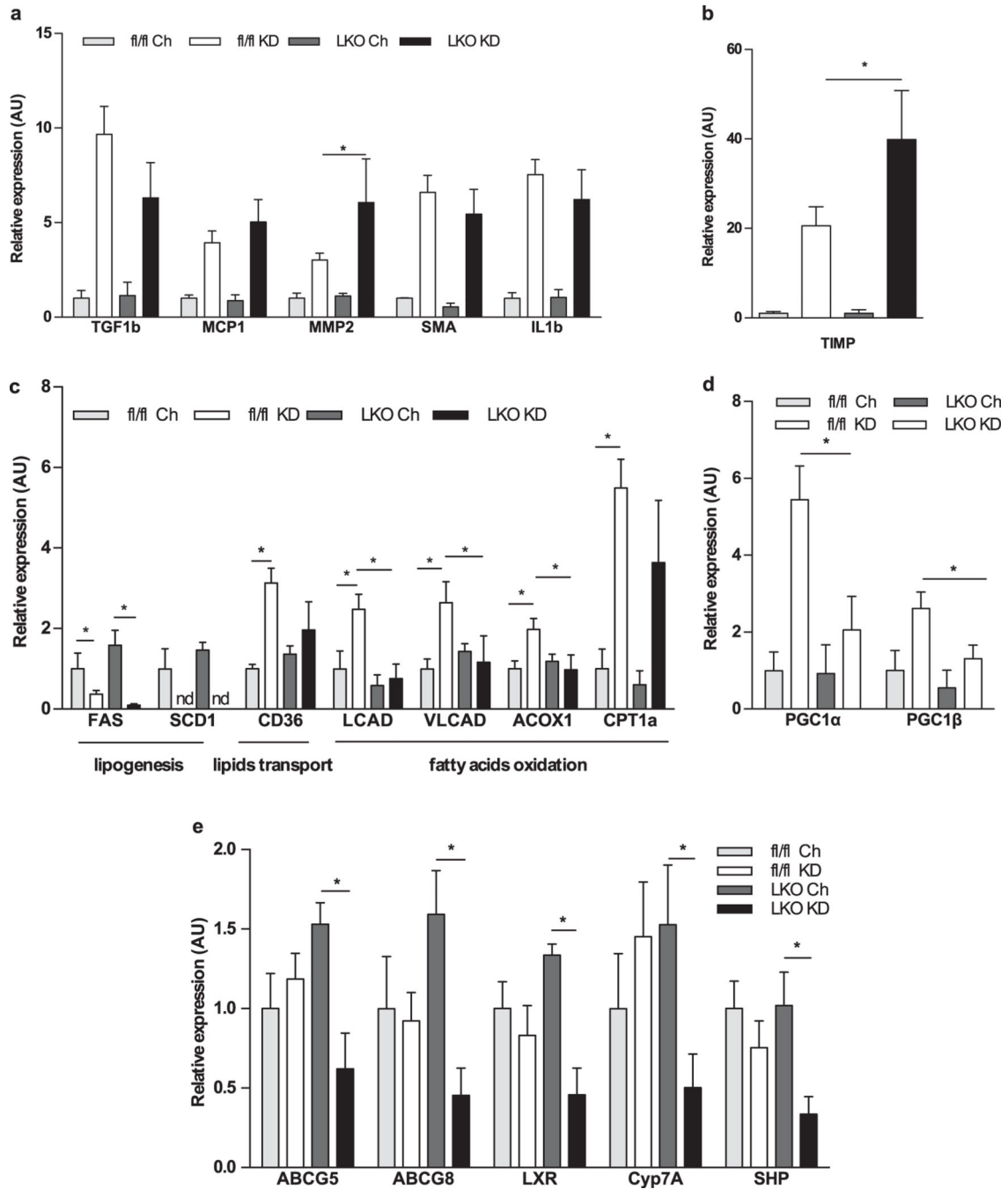


Figure 3.

Progressive liver injury and hepatic fat accumulation is observed in LKO mice. **a** KD-fed LKO mice have heavier liver to body weight ratio. **b** Histological analysis revealed progressive hepatic injury and lipid accumulation in LKO mice with increased lipid accumulation, inflammation and ballooning compared to chow fed mice (panels I, III, V, VII stained by H&E, at 20x magnification). Mild fibrosis is also seen as assessed by Sirius Red (SR) staining (panels II, IV, VI, VIII at 20x magnification). **c** Quantification of histopathology scores in f/fi vs LKO mice is shown. **d** Hepatic triglycerides are comparably increased in all KD fed mice. **e** A selective increase in hepatic cholesterol accumulation is seen in LKO mice fed with KD. *N* = 6–8 mice/group

**Figure 4.**

LKO mice show liver gene expression suggestive of inflammation, fibrosis, and altered lipid metabolism. **a, b** Markers for inflammation and fibrosis, such as MMP2 and TIMP1, are increased in LKO mice compared to fl/fl mice consuming KD. However, most genes are equally induced by KD in all mice. **c** Hepatic gene expression markers of de novo lipogenesis are reduced with KD consumption. Genes involved in fatty acid oxidation and lipid transport have attenuated induction in KD-fed LKO mice. **d** Similarly, PGC-1 α and

PGC-1 β genes have reduced expression in these mice. **e** Genes involved in cholesterol biliary excretion also have impaired induction in KD-fed LKO mice. *N*= 6–8 mice/group

Author Manuscript

Author Manuscript

Author Manuscript

Author Manuscript

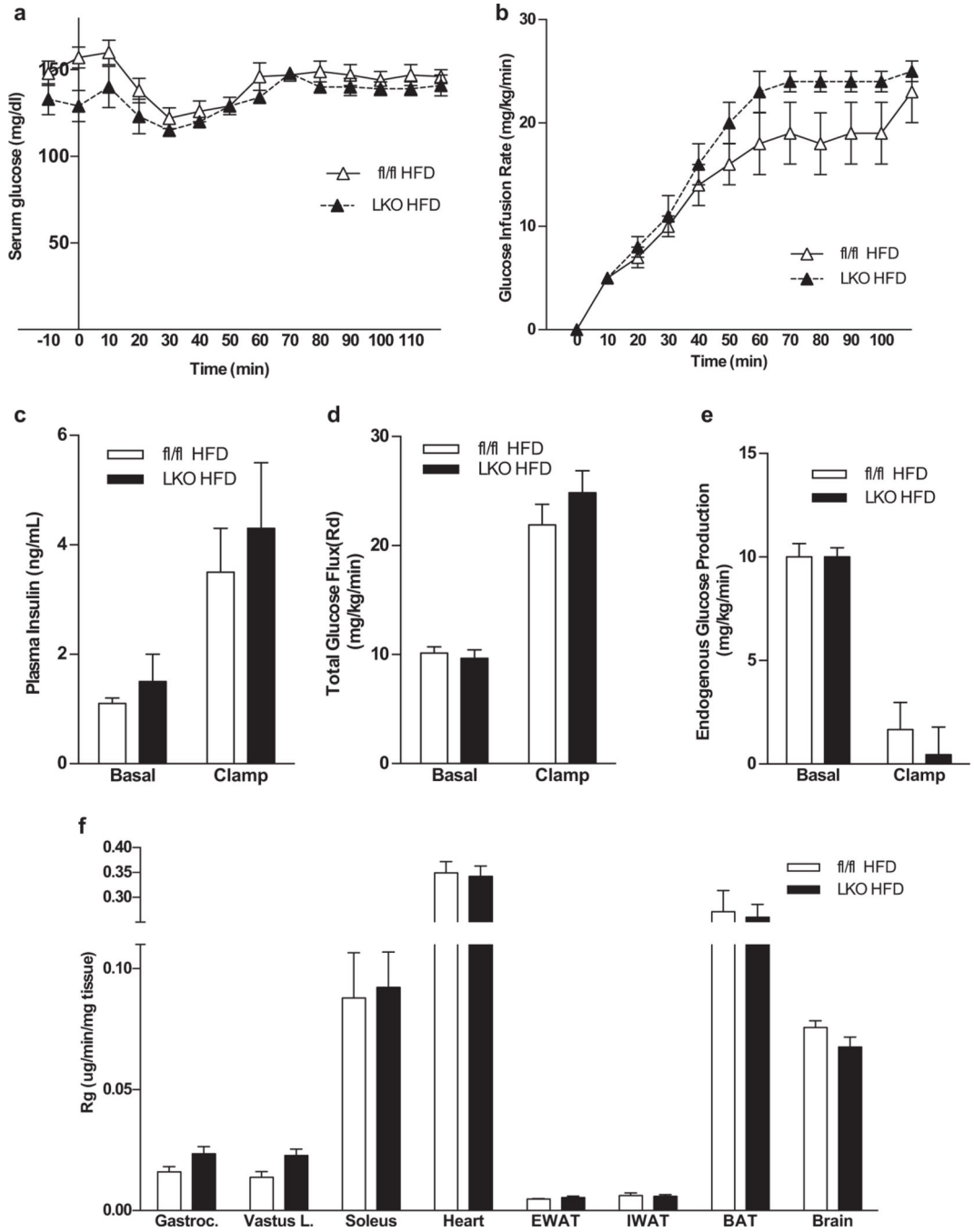


Figure 5. Glucose metabolism is not impaired in LKO mice fed a high-fat diet. Arterial glucose concentration (a), glucose infusion rate (b), plasma insulin (c), total glucose flux (d), suppression of hepatic glucose production (e) and tissue (soleus, gastrocnemius, superficial vastus lateralis (SVL), heart, and brain) glucose uptake (f), during a hyperinsulinemic—euglycemic clamp in chronically catheterized 5-h fasted obese fl/fl and LKO mice. *N* = 6 mice/group

Table 1.

Circulating Metabolic Parameters in ad lib fed mice consuming chow or ketogenic diet. Data are mean±SEM. LKO, Liver specific FGF21 knockout; KD, ketogenic diet, fl/fl, flox/flox. Significance $p < .05$ by ANOVA.

Metabolite	Chow-fed		KD-Fed	
	fl/fl	LKO	fl/fl	LKO
β -Hydroxybutyrate (mM)	0.15±0.02 ^{c,d}	0.15±0.01 ^{c,d}	1.56±0.2 ^{a,b}	1.49±0.27 ^{a,b}
Triglycerides (mg/dL)	58.14±7.47	82.18±18.26 ^c	43.91±4.96 ^b	75.27±16.34
Cholesterol (mg/dL)	92.02±7.64 ^d	108.2±13.69 ^d	96.04±12.57 ^d	144.24±15.56 ^{a,b,c}
Glucose (mg/dL)	175.3±8.8 ^{c,d}	168.9±9.5 ^{c,d}	119.4±18.6 ^{a,b}	126.6±19.6 ^{a,b}
Insulin (ng/mL)	0.66±0.17 ^{c,d}	0.64±0.26 ^{c,d}	0.12±0.05 ^{a,b}	0.17±0.03 ^{a,b}
ALT (IU/L)	14.54±0.24 ^d	12.57±2.3 ^d	27.86±4.42	35.15±4.94 ^{a,b}

^aSignificantly different from Chow fed WT;

^bSignificantly different from Chow fed LKO;

^cSignificantly different from KD fed WT;

^dSignificantly different from KD fed LKO;